Article

Cell Reports

Tumor-Derived Mesenchymal Stem Cells Use Distinct Mechanisms to Block the Activity of Natural Killer Cell Subsets

Graphical Abstract

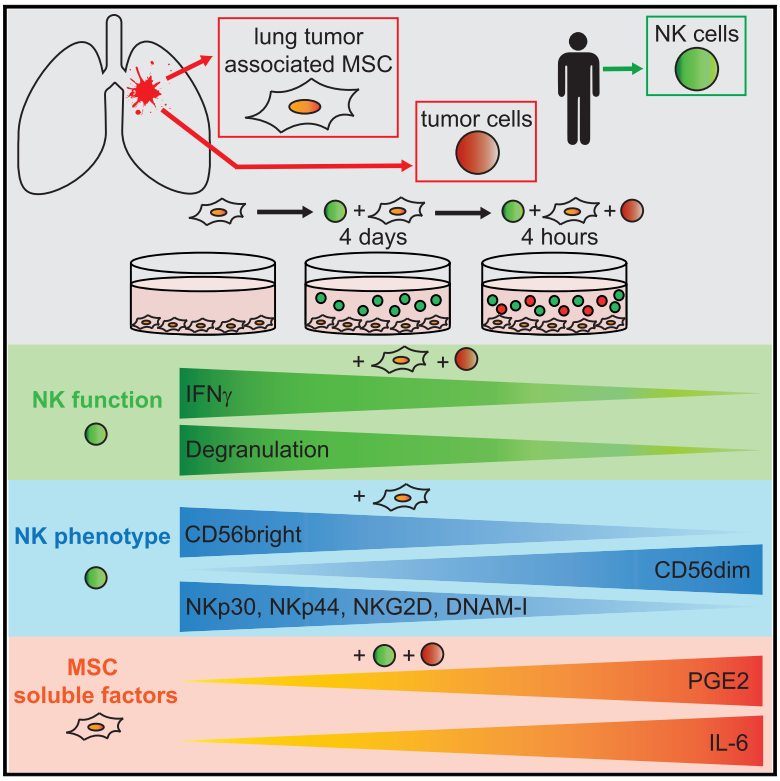

Highlights

- Lung-tumor-derived MSCs (T-MSCs) reduce NK cell function and modulate NK phenotype
- T-MSCs are more immunosuppressive than their non-tumor-associated counterparts
- CD56 dim/bright and functional NK cell subsets are differentially modulated by MSCs
- Modulation of NK cell function and phenotype by MSCs occurs mainly through PGE2

Authors

Sabine Galland, Joanna Vuille, Patricia Martin, Igor Letovanec, Anne Caignard, Giulia Fregni, Ivan Stamenkovic

Correspondence

ivan.stamenkovic@chuv.ch

In Brief

Galland et al. compare natural killer (NK) cell immunosuppression by mesenchymal stem cells (MSCs) from primary human squamous cell carcinomas and adjacent normal lung tissue. Tumor-associated MSCs exert stronger immunosuppression than normal-tissue-derived MSCs and modulate different NK functions by distinct mechanisms.

Galland et al., 2017, Cell Reports *20*, 2891–2905
September 19, 2017
http://dx.doi.org/10.1016/j.celrep.2017.08.089

CellPress

Cell Reports
Article

Tumor-Derived Mesenchymal Stem Cells Use Distinct Mechanisms to Block the Activity of Natural Killer Cell Subsets

Sabine Galland,[1] Joanna Vuille,[1] Patricia Martin,[1] Igor Letovanec,[1] Anne Caignard,[2] Giulia Fregni,[1,3] and Ivan Stamenkovic[1,3,4,*]
[1]Experimental Pathology Service, Institute of Pathology, CHUV, Faculty of Biology and Medicine, University of Lausanne, Rue du Bugnon 25, 1011 Lausanne, Switzerland
[2]INSERM 1160, Institut Universitaire d'Hématologie, Hôpital Saint Louis, 1, Avenue Claude Vellefaux, 75010 Paris, France
[3]Senior author
[4]Lead Contact
*Correspondence: ivan.stamenkovic@chuv.ch
http://dx.doi.org/10.1016/j.celrep.2017.08.089

SUMMARY

Mesenchymal stem cells (MSCs) display pleiotropic functions, which include secretion of soluble factors with immunosuppressive activity implicated in cancer progression. We compared the immunomodulatory effects on natural killer (NK) cells of paired intratumor (T)- and adjacent non-tumor tissue (N)-derived MSCs from patients with squamous cell lung carcinoma (SCC). We observed that T-MSCs were more strongly immunosuppressive than N-MSCs and affected both NK function and phenotype, as defined by CD56 expression. T-MSCs shifted NK cells toward the $CD56^{dim}$ phenotype and differentially modulated $CD56^{bright/dim}$ subset functions. Whereas MSCs affected both degranulation and activating receptor expression in the $CD56^{dim}$ subset, they primarily inhibited interferon-γ production in the $CD56^{bright}$ subset. Pharmacological inhibition of prostaglandin E2 (PGE2) synthesis and, in some MSCs, interleukin-6 (IL-6) activity restored NK function, whereas NK cell stimulation by PGE2 alone mimicked T-MSC-mediated immunosuppression. Our observations provide insight into how stromal responses to cancer dampen NK cell activity in human lung SCC.

INTRODUCTION

Lung cancer is the second most common malignancy and the leading cancer in terms of lethality worldwide. More than 85% of cases fall into the non-small-cell lung cancer (NSCLC) class, which is associated with a predicted 5-year survival of 17.8% and whose predominant histological subtypes are adenocarcinoma (~50%) and squamous cell carcinoma (SCC) (~40%; Chen et al., 2014). The tumor microenvironment provides a wide range of resources that support NSCLC progression (Wood et al., 2014), among which are diverse stromal cells, including activated mesenchymal stem cells (MSCs) (Bussard et al., 2016; Raffaghello and Dazzi, 2015).

Although they were initially described in the bone marrow (BM), MSCs display a broad tissue distribution and are found in adipose, synovial, and lung tissue as well as in umbilical cord and peripheral blood (Williams and Hare, 2011). MSCs are a heterogeneous stromal cell population defined based on three functional and phenotypic criteria: adherence to plastic; expression of selected and lack of lineage-specific cell surface markers; and the capacity to differentiate toward a variety of mesenchymal lineages (Dominici et al., 2006). Among a plethora of effector functions, MSCs have been reported to exert immunosuppressive activity after priming by cytokines from a pro-inflammatory microenvironment, particularly interferon-γ (IFN-γ), tumor necrosis factor α (TNFα), and interleukin-1β (IL-1β) or through toll-like receptor (TLR) stimulation (Bernardo and Fibbe, 2013; Dumitru et al., 2014; Krampera, 2011). Following activation, the spectrum of MSC immunosuppressive activity in humans includes secretion of human leukocyte antigen (HLA-G), transforming growth factor β (TGFβ), prostaglandin E2 (PGE2), tumor necrosis factor alpha-inducible protein 6 (TNFAIP6/TSG-6), heme oxygenase 1 (HO-1/HMOX1), IL-10, IL-6, indoleamine 2,3-dioxygenase 1 (IDO1), hepatocyte growth factor (HGF), and leukemia inhibitory factor (LIF) as well as programmed death ligand (PD-L1/2) and Fas ligand (FasL) signaling (Poggi and Giuliani, 2016; Poggi et al., 2014; Spaggiari and Moretta, 2013; Stagg and Galipeau, 2013; Turley et al., 2015; Uccelli et al., 2006; Le Blanc and Davies, 2015). The immunosuppressive effects of MSCs require proximity to their target cells, which include T and B lymphocytes as well as natural killer (NK) cells (Aggarwal and Pittenger, 2005; Uccelli et al., 2008).

As a first line of defense against tumors and pathogens, NK cells patrol tissues and can exert antitumor immunosurveillance by secreting cytokines, including IFN-γ, TNFα, and IL-10, and releasing cytotoxic granules whose contents kill tumor cells. Not surprisingly, NK cell infiltration of tumor tissue correlates with better prognosis in diverse cancer types, including lung carcinomas (Platonova et al., 2011; Villegas et al., 2002), and low NK cell activity is associated with increased cancer risk in adults (Imai et al., 2000). NK cell detection of and response to target cells are regulated by cell surface activating and inhibitory receptors. Activation of NK cells therefore requires integration of signals from their target cells that may be subject to modulation

A

	Patient 1	Patient 2	Patient 3	Patient 4	Patient 5
Tumor type	Moderately to poorly differentiated invasive SCC	Poorly differentiated SCC	Moderately differentiated keratinizing SCC, partially sarcomatoid	Poorly differentiated SCC, basaloid subtype	Moderately differentiated SCC, with focal keratinization
TNM	pT2b N0 (0/14) Mx	pT2a pN0 (0/20) R0	pT3 pN9 (0/35) Mx R0	pT2a pN0 (0/8)	pT2a pN0 (0/7) pL0 R0
Sex	Female	Female	Male	Male	Male
Age	79	64	70	83	74
Smoking history	Yes	Yes	Yes	Yes	Yes
Neoadjuvant	No	No	No	No	No

SCC: squamous cell carcinoma; p: pathological classification; T: primary tumor; N: node; M: metastasis; X: not assessed histologically; R: residual tumor; L: lymphatic invasion. pTNM classification following the criteria of «The TNM Classification of Malignant Tumours, 8th Edition, UICC», edited by Prof. James Brierle, Wiley Blackwell, 2016.

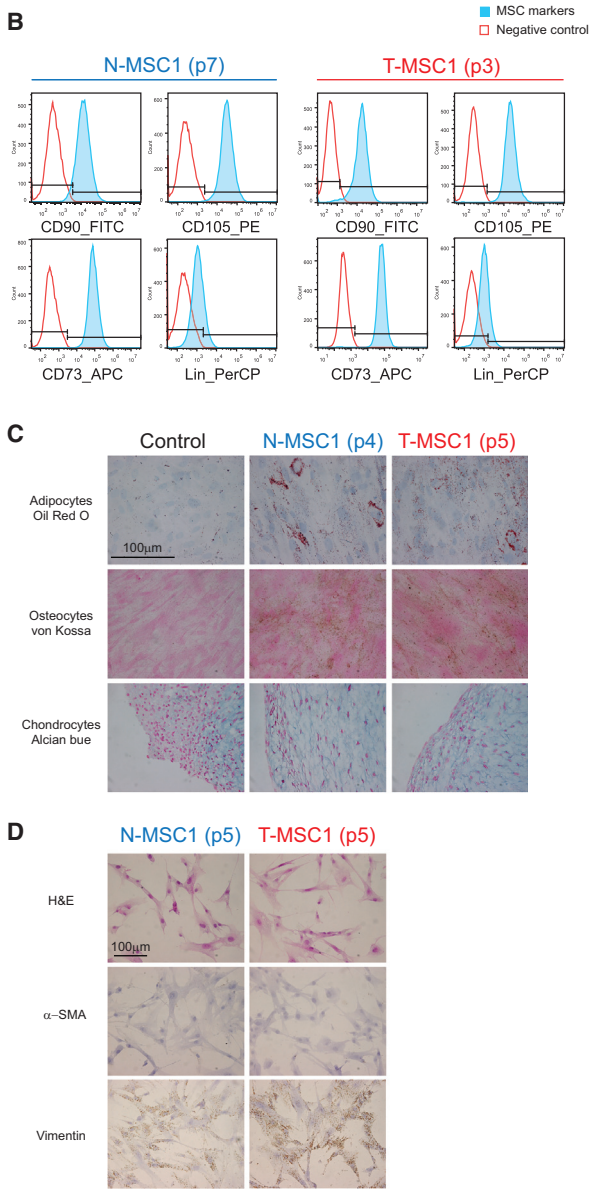

Figure 1. Clinical Data and MSC Characterization

(A) Clinical data related to the five patients. See also Table S1.

(B–D) Characterization of N- and T-MSCs from one representative patient. (B) Expression of CD90, CD105, CD73, and lineage (Lin: anti-CD14, -CD20, -CD34, and -CD45 antibody cocktail) markers by flow cytometry is shown. Cell passage (p) is shown in brackets. Cells stained with isotype-matched antibodies provided the negative control. (C) Adipogenic (Oil red O), osteogenic (Von Kossa), and chondrogenic (Alcian blue) MSC differentiation potentials are shown. Cells cultured in standard medium provided the control condition. The scale bar represents 100 μm. (D) H&E, α-SMA, and vimentin IHC stainings are shown. The scale bar represents 100 μm.

by diverse cell types, including MSCs (Moretta et al., 2001; Spaggiari et al., 2008; Vivier et al., 2008).

NK cell function correlates with CD56 expression, where high ($CD56^{bright}$) and low ($CD56^{dim}$) expression are associated with elevated cytokine production and high degranulation potential, respectively (Caligiuri, 2008; Cooper et al., 2001; Lanier et al., 1986). NK cells are found in the stroma of human lung tumors (Jin et al., 2014), where they primarily display a $CD56^{dim}$ phenotype, low expression of multiple activating receptors (Platonova et al., 2011; Vitale et al., 2014), and reduced function (Cremer et al., 2012; Gillard-Bocquet et al., 2013; Hodge et al., 2014; Pross and Lotzová, 1993).

Bone-marrow-derived MSCs (BM-MSCs) can inhibit NK cell proliferation, cytotoxicity, and cytokine production by secreting IDO1, TGFβ, HLA-G, and PGE2 (Casado et al., 2013; Krampera et al., 2006; Rasmusson et al., 2003; Spaggiari et al., 2008). However, they can also be lysed by activated NK cells, depending on their expression of activating NK receptor ligands, including MHC class I polypeptide-related sequence (MICA, B), UL16 binding proteins (ULBPs), CD112, and CD155 (Poggi et al., 2005; Spaggiari et al., 2006, 2008). Most of our understanding of the functional MSC-NK cell relationship stems from experiments using normal BM-MSCs, peripheral blood NK cells, and tumor cell lines. In tumors, however, MSCs may become constituents of the tumor niche and display distinct features from those of MSCs derived from healthy tissues or the BM (DelaRosa et al., 2012; Di Trapani et al., 2013; Gottschling et al., 2013; Johann et al., 2010; Liu et al., 2014).

Here, we provide insight into the effect of tumor-associated MSCs on NK cell activity by comparing the immunomodulatory activity toward freshly isolated NK cells from healthy donors of paired samples of MSCs isolated from tumor tissue (T-MSCs) and normal adjacent lung tissue (N-MSCs) of patients with squamous cell lung carcinoma. We observed marked differences between T- and N-MSCs, from their phenotype to their immunosuppressive function. Despite the ability of MSCs to secrete a variety of mediators with immunosuppressive effects, T-MSCs could mediate inhibition of NK cell function primarily through PGE2. Our observations provide insight into how stromal responses to cancer growth blunt NK cell activity in human lung SCC.

RESULTS

Characterization of MSCs Isolated from Patients with Lung SCC

Stromal cells were isolated from dissociated primary lung SCC (Figure 1A) as well as from adjacent non-tumor tissue from five patients and verified for functional and phenotypic MSC features as defined by the International Society for Cellular Therapy (ISCT) (Dominici et al., 2006). Accordingly, both tumor and

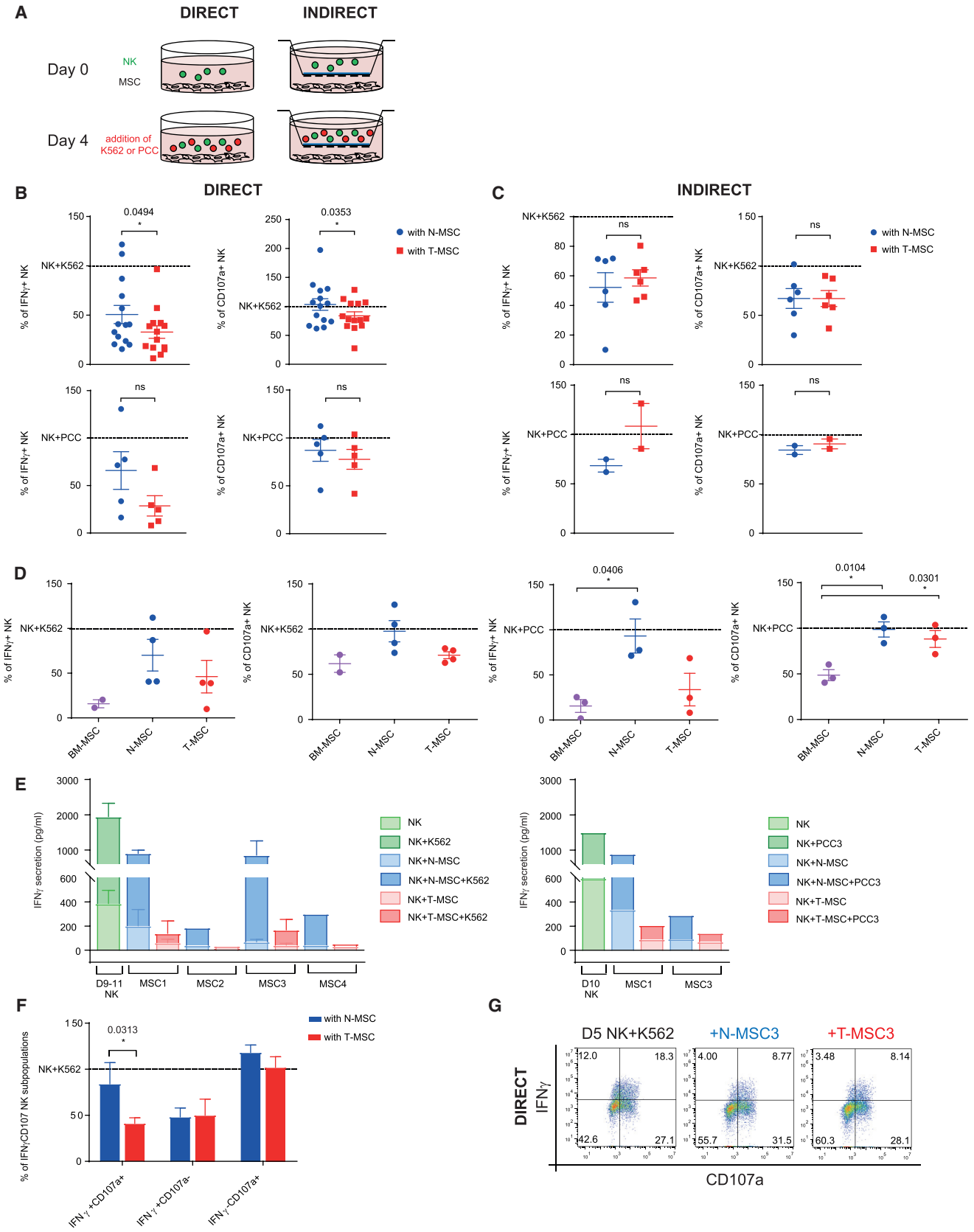

(legend on next page)

tumor-free lung-tissue-derived stromal cells, which we selected for our study, were adherent to plastic under standard culture conditions; expressed comparable levels of CD105, CD73, and CD90 and lacked expression of lineage markers (Figure 1B); and underwent differentiation to osteocytes, adipocytes, and chondrocytes in vitro in response to appropriate stimulation (Figure 1C). Because of the uncertainty as to the distinction between tumor-associated MSCs and myofibroblasts, often termed cancer-associated fibroblasts (CAFs) (Kalluri, 2016), we assessed the expression of the intermediate filament vimentin, a marker of mesenchymal cells, and α-smooth muscle actin (α-SMA), a hallmark of myofibroblasts (Desmoulière et al., 2004) in our stromal cells. Immunohistochemical (IHC) analysis using specific anti-vimentin and anti-α-SMA antibodies revealed that, as expected, the majority of MSCs expressed vimentin but displayed undetectable levels of α-SMA (Figure 1D).

Immunophenotype of Tumor-Infiltrating Cells and Primary Cancer Cell Characterization

Untreated, surgically removed primary lung tumors from five patients with a smoking history were subjected to histological analysis and diagnosed as moderately to poorly differentiated, invasive SCC (TNM pT2-pT3; Figure 1A; Table S1). Immune cell tumor infiltrates were assessed by immunostaining of tissue sections from four patients for CD3, CD4, CD8, CD20, CD68 KP1, Granzyme B, CD56, PD-L1, PD1, and FoxP3 (Table S1) and by flow cytometry of cells from three of the tumors (patients 1, 2, and 5). NK cells constituted less than 1% of the total $CD45^+$ cell infiltrate in all three tumors (0.2% of $CD45^+$ cells for patient 1, 0.59% for patient 2, and 0.55% for patient 5). The relative abundance of T cells ($CD4^+$, $CD8^+$, and $FoxP3^+CD25^+$ T reg cells), B cells, and myeloid cells was variable among the samples, reflecting IHC staining (Figure S1; Table S1).

Primary cancer cells (PCC) from three of the patients (patients 2, 3, and 4) were obtained by culturing single cells from the tumor bulk in ultra-low attachment flasks and in knockout (KO) medium supplemented with growth factors. Cells were selected for their ability to form spheres in culture and tested for tumorigenicity following injection beneath the kidney capsule of NOD-SCID common γ-chain knock out (NSG) mice. We then addressed the potential of the PCC to become NK target cells by assessing their expression of NK activating receptor ligands (Figures S2A and S2B) and HLA class I molecules (Figure S2C) in comparison to that of the K562 leukemia cell line, a classical NK target.

Primary cells from lung SCC displayed lower expression of several NK cell ligands than the K562 cell line, including CD112 (*NECTIN2*), CD155 (*PVR*), and *ULBP1*. In contrast, expression of the NKG2D ligands *MICA* and *MICB* was higher than that of other ligands in PCC (Figure S2A) and comparable to their expression in K562 cells (Figure S2B). MICA and MICB are involved in NK cell activation by interacting with NKG2D (Jamieson et al., 2002), on the one hand, and in NK exhaustion upon extended stimulation on the other (Groh et al., 2002; Chretien et al., 2014; Oppenheim et al., 2005). HLA class I expression tended to increase over time in PCC co-cultured with NK cells (Figures S2Ci and S2Cii), which may provide a mechanism of resistance to NK cell killing. Although PCC appeared to display a phenotype that is less prone to induce NK activation than that of K562 cells, they were nevertheless able to stimulate NK cell degranulation at different effector:target ratios (Figure S2D). Thus, primary lung SCC cells are sensitive to NK-mediated immunosurveillance.

T-MSCs Suppress the NK Cell Response to K562 and Primary SCC Cells More Strongly Than N-MSCs

The effect of T- and N-MSCs on NK cell function was investigated in direct and indirect (Transwell) co-culture conditions (Figure 2A). Freshly isolated NK cells were cultured with T- and N-MSCs for 4 days, following which their activation by tumor cells was assessed in a 4-hr assay. NK cells from different donors displayed variable activation in response to K562 cells and PCC (Figure S3A). Nevertheless, in direct co-culture,

Figure 2. T-MSCs Are More Immunosuppressive Than N-MSCs Toward the NK Response to K562 and PCC

(A) Schematic representation of direct and indirect co-culture experiments.

(B, C, D, and F) NK cell activation (percentages of CD107a and intracellular IFN-γ-positive cells) by K562 or PCC cells following N-, T-, and BM-MSC co-culture, as assessed by flow cytometry. Results were normalized to those of NK cells cultured without MSCs for the same duration and activated by target cells (the control condition is represented by the horizontal dashed line). Results show the mean ± SEM.

(B) Direct co-cultures. Graphs plot individual values of 8 independent experiments with K562 cells (eight different NK cell donors; MSC1 [n = 3 biological replicates]; MSC2 [n = 2]; MSC3 [n = 6]; MSC4 [n = 2]; MSC5 [n = 1]) and 3 experiments with PCC (three NK cell donors; MSC1 [n = 1]; MSC2 [n = 1]; MSC3 [n = 2]; MSC4 [n = 1]).

(C) Indirect co-cultures. Two experiments were done with K562 cells (two NK cell donors; MSC1 [n = 2]; MSC2 [n = 1]; MSC3 [n = 2]; MSC4 [n = 1]) and one with PCC (one NK cell donor; MSC1 [n = 1]; MSC3 [n = 1]).

(D) Comparison of the effects of BM-MSCs to those of lung tissue MSCs. Graphs plot individual values of two experiments in direct MSC-NK co-culture with K562 (two different NK cell donors; MSC2 [n = 1]; MSC3 [n = 2]; MSC4 [n = 1]; BM-MSC [n = 2]) and 2 experiments with PCC (PCC2, 3, and 4; two NK cell donors; MSC2 [n = 1]; MSC3 [n = 1]; MSC4 [n = 1]; BM-MSC [n = 3]).

(E) IFN-γ secretion (pg/mL) by NK cells co-cultured with N- (blue bar) and T-MSCs (red bar) before and after activation by tumor cells (K562, left panel, and PCC, right panel). IFN-γ secretion by NK cells cultured alone is shown in green. Light color bars, basal NK cell secretion (without tumor cells); dark color bars, secretion after activation. Mean values ± SEM for 3 experiments with K562 as target cells (three NK cell donors; MSC1 [n = 2]; MSC2 [n = 1]; MSC3 [n = 3]; MSC4 [n = 1]) and one experiment with PCC as target cells (one single NK cell donor; MSC1 [n = 1] and 3 [n = 1]) are shown.

(F) Percentages of $IFN\text{-}\gamma^{+/-}CD107a^{+/-}$ NK cell subpopulations after 4 days of co-culture with MSCs in 5 independent experiments using NK cells from 5 donors and MSCs from one patient (MSC3; n = 6).

(G) Representative flow density dot plots showing expression of IFN-γ and CD107a by K562-activated NK cells in direct co-culture with and without MSCs (single NK cell donor; MSC3).

Statistical significance was determined by Wilcoxon matched-pairs signed rank test (pairing on MSC patient; B, C, and F) or unpaired t test with Welch's correction (D; * indicates significance at $p < 0.05$; **$p < 0.01$; ns, not significant). See also Figure S3.

T-MSCs were consistently and significantly more immunosuppressive than N-MSCs toward NK cells exposed to K562 cells, as assessed by IFN-γ production and CD107a (lysosomal-associated membrane protein-1) expression, commonly used as a marker of degranulation (Alter et al., 2004; Figures 2B and S3Bi). Following activation by PCC, production of IFN-γ as well as degranulation were slightly, but not significantly, more reduced in the presence of T-MSCs than in that of N-MSCs (Figures 2B and S3Bi). T-MSCs also exerted stronger suppression of IFN-γ production than of degranulation (Figure 2B).

In indirect co-culture, T-MSCs were less immunosuppressive than in direct co-culture and their inhibition of NK cell IFN-γ production and degranulation was comparable to that of N-MSCs (Figures 2C and S3Bii). In contrast to direct co-culture, NK cell production of IFN-γ in response to PCC was more strongly inhibited by N- than by T-MSCs. Thus, the robust immunosuppressive activity of T-MSCs toward NK cells appeared to be contact dependent and effective in the presence of both K562 cells and PCC. Because the immunosuppressive potential of MSCs has thus far been studied mainly using BM-MSCs, we included one sample isolated from an adult healthy donor as a reference for MSC-mediated NK inhibition. Bone marrow MSCs displayed strong inhibitory activity toward both IFN-γ production and degranulation by NK cells (Figure 2D) that was more closely reminiscent of T- than of N-MSCs.

Inhibition by MSCs (T-MSC > N-MSC) of intracellular IFN-γ production was reflected at the secretory level (Figure 2E, dark bars). Moreover, the inhibition was observed even before NK cell activation by K562 cells and PCC (Figure 2E, light bars). Similar to IFN-γ secretion, TNFα secretion by NK cells after activation by K562 cells was inhibited in the presence of MSCs and more strongly so in that of T- than of N-MSCs. Although the inhibition was less marked when K562 cells were substituted by PCC, the tendency was similar (Figure S3C).

We next interrogated the response to T- and N-MSCs of the different functional NK cell subpopulations, including IFN-γ^+CD107a$^+$ double-positive, IFN-γ^+CD107a$^-$ single-positive, and IFN-γ^-CD107a$^+$ single-positive cells (Figures 2F, 2G, and S3D). The strongest and most selective inhibition by T-MSCs was observed in the NK double-positive subpopulation. The IFN-γ^+CD107a$^-$ single-positive subpopulation was equally inhibited by N- and T-MSCs, whereas the IFN-γ^-CD107a$^+$ single-positive NK subpopulation was virtually unaffected (Figure 2F). Thus, the NK subpopulations that are the most strongly inhibited by MSCs, particularly in direct co-culture, are those capable of secreting IFN-γ (Figures 2F and 2G).

T-MSCs Downregulate NK-Cell-Activating Receptors and Induce the CD56^{dim} NK Cell Phenotype

To understand how MSCs downregulate NK cell function, we interrogated NK receptor modulation in the presence of T- and N-MSCs. MSCs (T-MSC > N-MSC) inhibited cell surface expression of the NK receptors NKp44, NKp30, NKG2D, DNAM-I, and NKG2A (Figure 3Ai). Differences between the inhibitory effects of N- and T-MSCs were significant for NKG2D, DNAM-I, and NKG2A receptors. Interestingly, their expression was affected only in direct contact with MSCs (Figure 3Ai), with the exception of NKp44, whose expression was partially inhibited in indirect co-culture (Figure 3Aii).

Surprisingly, we observed marked changes in the CD56$^{bright/dim}$ ratios of NK subpopulations in response to MSCs. In the absence of MSCs and after 4 days of exposure to IL-2, NK cells were predominantly CD56^{bright}. However, an inversion in the CD56$^{bright/dim}$ NK cell ratio was observed in direct co-culture with MSCs (Figures 3Bi and 3C) that was largely contact dependent (Figures 3B and 3C).

CD56^{bright} and CD56^{dim} NK Subpopulation Function Is Differentially Modulated by MSCs

In functional assays where NK cells are activated by tumor cells, the presence of MSCs, particularly T-MSCs, also tipped the balance toward the CD56^{dim} NK phenotype in a contact-dependent manner (Figure 4A). Functional comparison revealed that BM-MSCs were more closely related to T-MSCs than to N-MSCs, as demonstrated by their robust induction of the CD56^{dim} NK subset after activation by K562 cells (Figure 4Bi) and PCC (Figure 4Bii).

Interestingly, inhibition of NK cell function exerted by MSCs differed between the CD56$^{dim/bright}$ subpopulations. In control conditions (NK cells cultured with K562 cells alone), the CD56^{bright} NK cell subset (Figure 4C, first line), associated with elevated cytokine production, was dominant. Upon introduction of MSCs (Figure 4C, lines 2 and 3), the bulk NK cell population decreased its cytokine production and degranulation capacity. However, because the presence of MSCs increased the CD56^{dim} subpopulation, which was associated with degranulation, the change in function of the total NK cell population mostly reflected functional inhibition of the CD56^{dim} subset. Thus, MSC-mediated IFN-γ inhibition occurred predominantly in the CD56^{bright} subpopulation, whereas NK degranulation was inhibited by MSCs in the CD56^{dim} subtype. Inhibition of both functions, particularly cytokine production, was largely contact dependent (Figure 4C). The total NK cell population indirectly co-cultured with MSCs was mainly composed of CD56^{bright} cells, prone to cytokine secretion and comparable to NK cells activated by tumor cells without MSCs.

Modulation of NK receptors also differed between the CD56^{dim} and CD56^{bright} NK subsets. Thus, downregulation of NKp44, NKp30, NKG2D, and DNAM-I receptor expression occurred in the CD56^{dim} subpopulation, appeared to be highly contact dependent, and was more pronounced in the presence of T-MSCs than in that of N-MSCs (Figure 4D). In indirect co-culture, only NKp44 receptor expression was mildly inhibited, whereas NKG2D receptor expression was slightly increased. In the CD56^{bright} subset, only NKG2D expression was slightly decreased in direct co-culture with MSCs. With this exception, receptor expression in CD56^{bright} NK cells remained virtually unaffected by direct or indirect co-cultures with MSCs.

Inhibition of NK cell activating receptors (NKp44, NKp30, NKG2D, and DNAM-I) may provide the mechanism that underlies MSC-mediated dysfunction of CD56^{dim} NK cells. In contrast, inhibition of cytokine production in the CD56^{bright} subset was not associated with major changes in receptor expression, except for mild NKG2D downregulation in direct co-culture with MSCs (Figure 4D). We therefore interrogated the mechanisms involved

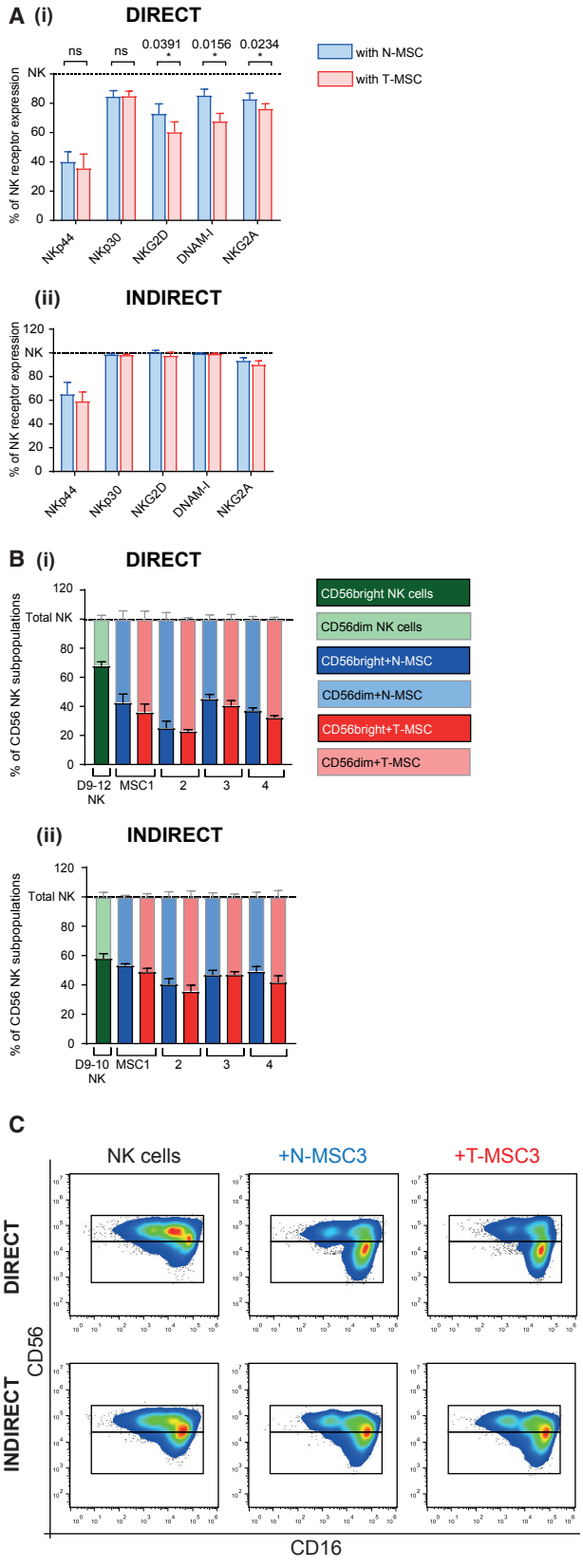

Figure 3. The NK Cell Phenotype Is Strongly Modulated by Direct Co-culture with N- and T-MSCs

(A and B) NK phenotype as assessed by flow cytometry after direct (i) and indirect (ii) co-cultures with N- or T-MSCs, normalized to control conditions (NK cells alone, horizontal dashed line). Mean values ± SEM are shown. (A) Expression of NK cell receptors is shown. (i) Data from 4 experiments are shown (four NK cell donors; MSC1 [n = 2]; MSC2 [n = 2]; MSC3 [n = 2]; MSC4 [n = 1]; MSC5 [n = 1]). (ii) Results from 2 experiments are shown (two NK cell donors; MSC1 [n = 2]; MSC2 [n = 1]; MSC3 [n = 2]; MSC4 [n = 1]). Data were analyzed using Wilcoxon matched-pairs signed rank test. (B) Percentages of $CD56^{bright}$ and $CD56^{dim}$ NK subpopulations in control conditions (NK cultured alone, green bar) and in co-culture with N- and T-MSCs are shown. Light tones depict the $CD56^{dim}$ NK subset, dark tones the $CD56^{bright}$ subset. (i) Results from 4 experiments are shown (four NK cell donors; MSC1 [n = 6]; MSC2 [n = 2]; MSC3 [n = 8]; MSC4 [n = 2]). (ii) Data from 2 experiments are shown (two NK cell donors; MSC1 [n = 6]; MSC2 [n = 3]; MSC3 [n = 6]; MSC4 [n = 3]). (C) Representative flow smooth contour plots (with outliers) showing CD16 and CD56 expression by NK cells in direct and indirect co-cultures with and without MSCs (single NK cell donor; MSC3).

in MSC-induced suppression of cytokine production in the $CD56^{bright}$ NK subset.

Expression of Immunosuppressive Mediators in T- and N-MSCs

First, we addressed the expression of genes implicated in immune regulation in T-, N-, and BM-MSCs, including *IDO1*, *IL10*, *TGFB1*, *TNFAIP6* (TSG6), *HMOX1*, *HLAG*, *IL6*, and *PTGS2* (COX-2; Figures 5A and S4A). Whereas *IDO1*, *IL10*, and *HLAG* transcripts were almost undetectable at day 0 in culture (data not shown), *IL6* and *PTGS2* were expressed at variable levels in T- and N-MSCs from different patients (Figures 5A and S4A). Expression of some of these genes differed between BM-MSCs and lung tissue MSCs (Figure S4A). Thus, *IL6* expression in BM-MSCs was lower than in most T-MSCs and *TNFAIP6* was almost undetectable (Figure S4A). Conversely, *TGFB1* and *PTGS2* were more highly expressed in BM-MSCs than in T-MSCs, with the exception of T-MSC1 (Figure S4A). T-MSCs from patients 2 and 5 expressed higher levels of *IL6* than their non-tumor-tissue-derived counterparts, whereas *PTGS2* expression was comparable in the two MSC subsets (Figure 5A). However, T- and N-MSCs displayed distinct secretion levels of IL-6 and PGE2 after 4 days in culture (even though the statistical values for the latter were not significant; Figure 5B), which could explain, at least in part, the differential impairment by the MSC subsets of NK cell function. Expression of *IL6* and *PTGS2* by T-MSCs increased over time in culture and was strongly induced by the presence of NK cells, whereas expression of *TGFB1* remained constant (Figure 5C). In co-culture with tumor-activated NK cells, MSCs secreted high levels of IL-6, TGFβ1, and HGF, but of the three cytokines, IL-6 was the most differentially secreted between T- and N-MSCs and more so in the presence of PCC-activated NK cells (Figure S4B). Comparison between BM- and lung tissue MSC secretion of IL-6 and PGE2 (Figure S4C) in direct co-culture with NK cells and following activation by tumor cells revealed lower secretion of IL-6 by BM-MSCs than by T-MSCs but comparable secretion of PGE2 by the two MSC populations. In addition, BM-MSCs bore similarities to lung tissue MSCs for *MICA* and *TLR3* expression but also a distinct profile with higher *TLR4* and lower *CD274*, *NECTIN2*,

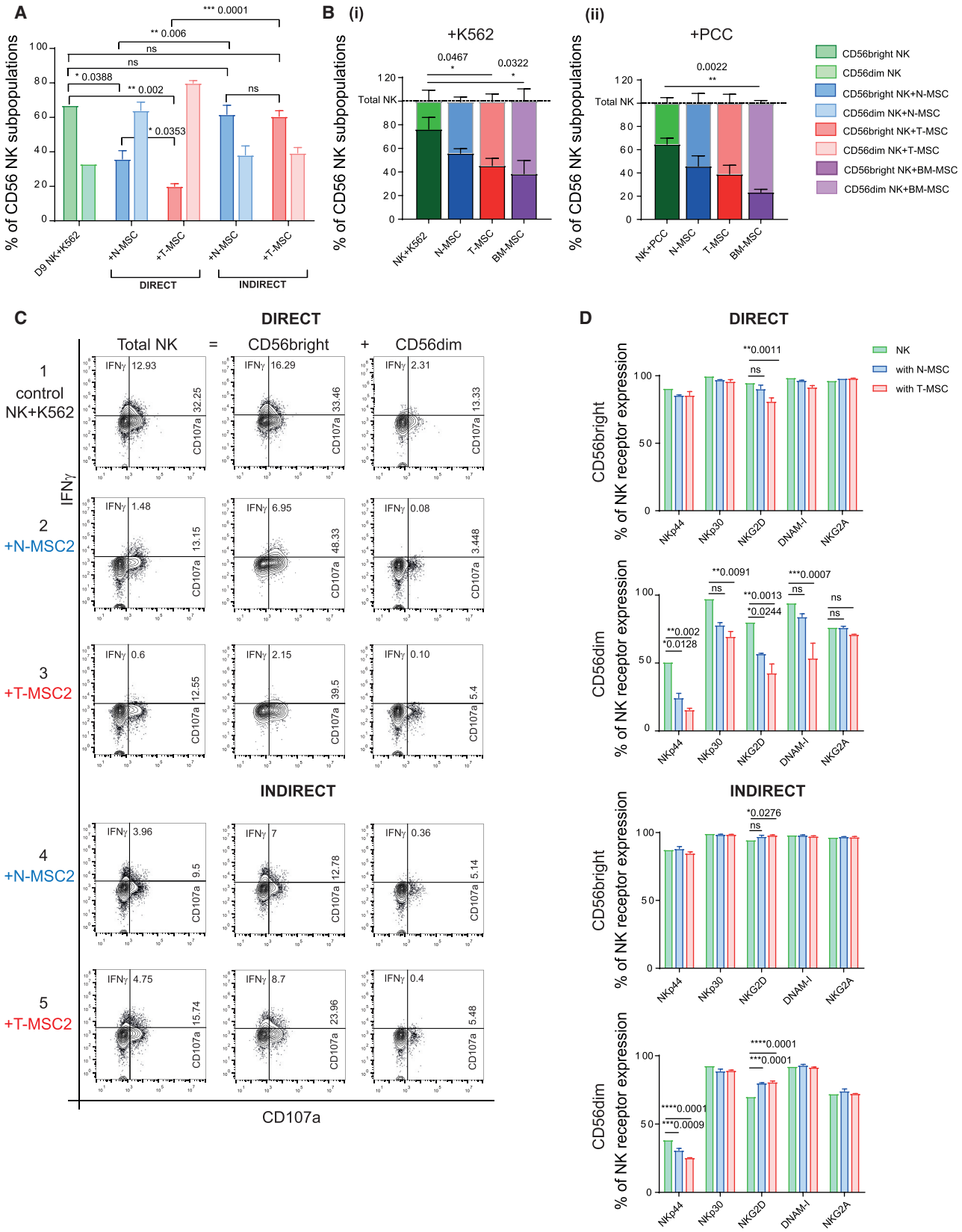

(legend on next page)

and *PVR* expression (Figure S4D). MSCs expressed low levels of NK-activating receptor ligands, except for the DNAM-I ligand *PVR* (CD155; Figures S4D and S4E).

IL-6 and PGE2 Are Implicated in T-MSC-Mediated Inhibition of NK Cell Function

Neutralization of IL-6 with a specific antibody (MAB206) and inhibition of COX-2 using a specific inhibitor (NS-398) were each partially effective in restoring NK function that had been suppressed by MSCs. However, the efficacy of the inhibitors appeared to be highly individual patient MSC dependent. COX-2 inhibition was the most effective in restoring NK cell function, whereas IL-6 had more heterogeneous effects. Analysis of co-culture supernatants demonstrated the level of inhibition reached using the inhibitors (Figure S5A). Interestingly, IL-6 inhibition increased PGE2 secretion (Figure S5Aiii).

Three experiments highlighted the heterogeneity of immunomodulatory mechanisms used by primary cells. In experiments using patient 2 MSCs, neutralization of IL-6 with antibody partially restored NK cell function, as measured by IFN-γ expression in response to K562 cells (Figure 6Ai). Similarly, inhibition of PGE2 synthesis using the COX-2 inhibitor NS-398 resulted in partial reversion of NK loss of IFN-γ expression induced by MSCs (Figure 6Ai). In contrast, neither inhibitor had a marked effect on NK cell degranulation (Figure S5Bi). Interestingly, rescue of NK cell cytokine expression resulting from inhibiting IL-6 and COX-2 function correlated with restoration of the $CD56^{bright}$ NK cell phenotype (Figures 6Aii and 6Aiii).

Surprisingly, in experiments with patient 5 MSCs (n = 2), addition of anti-IL-6 antibody did not restore NK cell function, whereas COX-2 inhibition partially reversed MSC-mediated blockade of IFN-γ expression and degranulation (Figures 6Bi and S5Ci). Nevertheless, COX-2 and IL-6 inhibition appeared to have a synergistic effect. Partial restoration of both NK cell cytokine production and degranulation by inhibition of MSC-derived immunosuppressive molecules was significantly correlated with an increase in the $CD56^{bright}$ NK cell phenotype (Figures 6Bii, 6Biii, and S5Cii).

We next investigated the mechanisms involved in the restoration of NK function and CD56 expression and assessed NK receptor expression. Addition of IL-6 inhibitor partially restored NKG2D expression in NK cells cultured with T-MSCs from patient 2 (Figure 6Ci). However, anti-IL-6 enhanced the inhibition of NKp30 and DNAM-I expression induced by T-MSCs. COX-2 inhibition increased NKp30 and NKp44 expression slightly and NKG2D expression more strongly. Neutralization of IL-6 from patient 5 MSCs had the same effect on NKG2D and NKp30 as its neutralization in patient 2 MSCs, increasing and decreasing their expression, respectively (Figure 6Cii). COX-2 inhibition partially restored NKp44, NKG2D, and NKp30 expression that had been downregulated by T-MSCs (Figure 6Cii). Combination of anti-IL-6 and the COX-2 inhibitor was comparable to the effect of the COX-2 inhibitor alone. Hence, COX-2 inhibitor administration to MSCs from both patients was effective in at least partially restoring IFN-γ production and NK receptor (NKG2D, NKp30, and NKp44) expression, whereas anti-IL-6 effects were patient MSC dependent.

We also assessed NK cell expression of CD25 (IL-2Rα) in co-cultures with MSCs, which was expressed by a small percentage of NK cells. In the presence of T-MSCs, CD25 was strongly downregulated, and its expression was partially and completely restored by anti-IL-6 antibody and COX-2 inhibitor, respectively (Figure 6D).

NK Stimulation with PGE2 Mimics T-MSC-Mediated IFN-γ Immunosuppression

To confirm the importance of MSC-mediated PGE2 secretion in NK cell inhibition, we stimulated NK cells with PGE2 in the absence of MSCs (donor 14 NK cells) at doses comparable to those secreted by T-MSCs in the presence of NK cells. PGE2 inhibited cytokine production by NK cells stimulated by K562 cells to a level comparable to that observed in T-MSC co-cultures (Figure 7A). In contrast, IL-6 stimulation did not affect NK function nor did it display synergy with PGE2 (Figure 7A). NK degranulation was unchanged after stimulation by PGE2, IL-6, or both, suggesting a role for PGE2 predominantly in the inhibition of cytokine production. Moreover, addition of PGE2 to NK cells increased the $CD56^{dim}$ subpopulation, as did the presence of T-MSCs (Figure 7B). Finally, stimulation with PGE2 alone was sufficient to reproduce the downregulation of NK receptors induced by T-MSCs (Figure 7C).

DISCUSSION

Using paired samples of primary MSCs isolated from lung SCC and adjacent tumor-free tissue, we showed that tumor-associated MSCs are more strongly immunosuppressive toward NK cells than their tumor-free tissue-derived counterparts, exerting

Figure 4. MSC Exert Different Effects on $CD56^{dim}$ and $CD56^{bright}$ NK Subsets

(A and B) Percentages of $CD56^{dim}$ and $CD56^{bright}$ NK cell subpopulations co-cultured with MSCs after 4 hr activation by tumor cells, assessed by flow cytometry. Light tones, $CD56^{dim}$ NK subset; dark tones, $CD56^{bright}$ subset. Tumor-activated NK cells cultured in the absence of MSCs provided a control (green bars). Results show the mean ± SEM. Statistical significance was determined by 2-way ANOVA followed by Tukey's multiple comparisons test. (A) Direct and indirect co-cultures with N- and T-MSCs after 4 hr activation by K562 cells are shown. Data are representative of a single experiment with pooled MSCs from 4 patients (MSC1-4) and a single NK cell donor. (B) Direct co-cultures with N-MSCs, T-MSCs, and BM-MSCs after 4 hr activation by K562 (i) or PCC cells (ii) are shown. Data representative of two experiments with pooled MSCs from 3 patients (MSC2-4), one donor of BM-MSCs, and two NK cell donors are shown. (i) Results from two experiments are shown (two NK cell donors; MSC2 [n = 1]; MSC3 [n = 2]; MSC4 [n = 1]; BM-MSC [n = 2]). (ii) Data from two experiments with PCC2, 3, and 4 are shown (two NK cell donors; MSC2 [n = 1]; MSC3 [n = 1]; MSC4 [n = 1]; BM-MSC [n = 2]).

(C) Representative dot plots showing the percentages of IFN-γ^+ and $CD107a^+$ cells in the total NK cell population and in the $CD56^{bright}$ and $CD56^{dim}$ subsets after direct and indirect co-cultures with MSCs from patient 2 and activation by K562 cells.

(D) Modulation of NK receptor expression in $CD56^{bright}$ and $CD56^{dim}$ subsets in direct and indirect co-cultures with MSCs compared to control conditions (NK cultured alone). Results show the mean ± SEM for a single experiment (single NK cell donor; MSC1 [n = 1] and 3 [n = 1]). Statistical significance was determined by 2-way ANOVA followed by Dunnett's multiple comparisons test with NK cells alone set as the control.

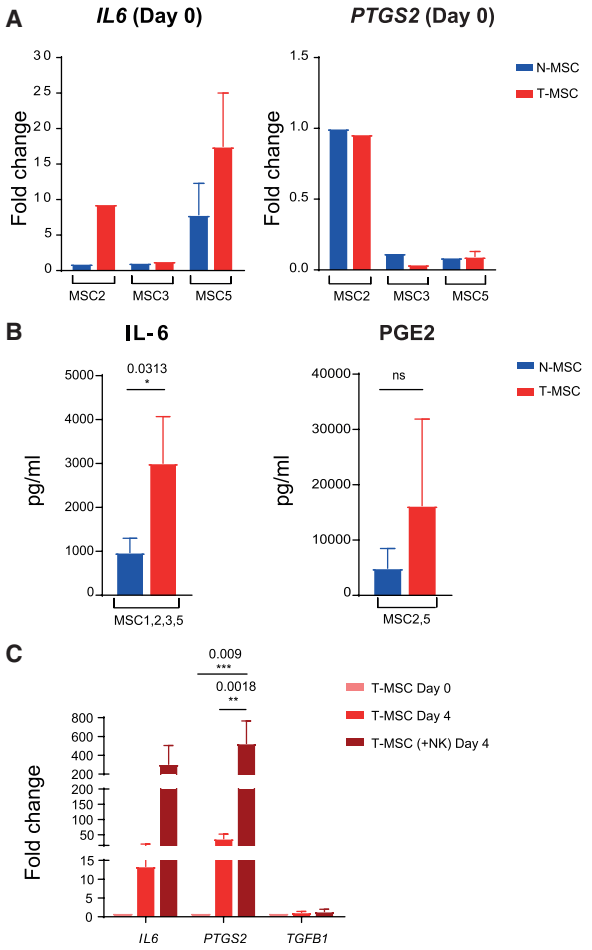

Figure 5. Differential Expression of Immune-Modulating Mediators by T- and N-MSCs

(A) Relative gene expression of *IL6* and *PTGS2* by N- and T-MSCs in the basal state (day 0 of co-culture) as assessed by qPCR and shown as a fold change in expression (N-MSC2 expression set as the control condition). Data are representative of four experiments (four NK cell donors; MSC2, 3, and 5), and results show the mean ± SEM.

(B) IL-6 and PGE2 secretion (pg/mL) by MSCs after 4 days in culture alone. Results show the mean ± SEM: MSC1, 2, 3, and 5 for IL-6 and MSC2 and 5 for PGE2. Statistical significance was determined by Wilcoxon matched-pairs signed rank test (* indicates significance at $p < 0.05$; **$p < 0.01$).

(C) Relative gene expression of *IL6*, *PTGS2*, and *TGFB1* by T-MSCs collected at the indicated time points with and without direct co-culture with NK cells (four NK cell donors; MSC2, 3, and 5). Results show fold change in gene expression compared to T-MSCs at day 0. Statistical significance was determined by 2-way ANOVA with Tukey's multiple comparisons test.

See also Figure S4.

stronger inhibition of NK cell IFN-γ secretion and degranulation in response to K562 and primary cancer cells. Functionally, T-MSCs were more closely related to BM-MSCs than N-MSCs. As two key functions of BM-MSCs are to participate in building a hematopoietic stem cell (HSC) niche and to protect HSCs from injury by mediators of inflammation and inflammatory effector cells, they must display potent immunosuppressive properties (Sotiropoulou et al., 2006; Spaggiari and Moretta, 2013; Spaggiari et al., 2008). In quiescent tissues, in the absence of inflammatory stimuli, MSCs may decrease or even temporarily lose their immunosuppressive features. However, in a tumor microenvironment, which mimics tissue repair and contains a vast array of cytokines derived from inflammatory, tumor, and activated stromal cells, MSCs may regain their full immunosuppressive potential and resemble their BM counterparts. The immunosuppressive mechanisms, as illustrated by the type and quantity of immunosuppressive cytokines produced and the level of NK cell receptor ligands expressed, may differ between BM- and T-MSCs, possibly as a function of the type of stimulatory microenvironment to which the cells are exposed.

MSCs, particularly T-MSCs, displayed markedly different degrees of inhibition of functional NK cell subpopulations, predominantly inhibiting NK cell subsets that produce IFN-γ. Because IFN-γ plays a prominent role in tumor rejection by preventing tumor stroma formation and tumor-induced angiogenesis (Zaidi and Merlino, 2011), as well as by activating the immune system, inhibition of its production by T-MSCs may be highly relevant toward facilitating tumor progression. Consistent with this notion, recent observations suggest that the predominant activity of NK cell subsets recruited to lung cancer is IFN-γ production rather than direct cancer cell killing (Carrega and Ferlazzo, 2017).

In addition to their production of IFN-γ, the activating receptor expression profile of NK cells was significantly affected by MSCs, with downregulation of NKp44, NKp30, NKG2D, DNAM-I, and NKG2A. MSCs also induced an inversion in the $CD56^{bright/dim}$ NK cell ratio in favor of the $CD56^{dim}$ phenotype. These effects were more pronounced in response to T-MSCs than to N-MSCs and, just like inhibition of IFN-γ production, were contact dependent. Consistent with these observations, intratumoral NK cells in human lung cancer display low expression of NKp30, CD56, NKG2D, and DNAM-I (Platonova et al., 2011; Esendagli et al., 2008; Levi et al., 2015).

The observed shift toward the $CD56^{dim}$ NK cell phenotype after exposure to MSCs is consistent with low expression of CD56 by NK cells in vivo (Esendagli et al., 2008; Platonova et al., 2011; Levi et al., 2015) and selective inhibition of the $CD56^{bright}$ subtype rather than expansion of the $CD56^{dim}$ subpopulation (Sotiropoulou et al., 2006). Following IL-2 stimulation, NK cells acquire a $CD56^{bright}$ phenotype, which correlates with an activated state of the cells in vitro. The $CD56^{dim}$ phenotype observed in the presence of MSCs therefore seems to reflect a decrease in NK cell activation, as suggested by our functional assays and by the reduced NK cell expression of IL-2Rα following T-MSC co-culture.

$CD56^{dim}$ and $CD56^{bright}$ NK cell functions were differentially modulated by MSCs. With the exception of NKG2D, T-MSCs downregulated activating receptor expression exclusively in the $CD56^{dim}$ NK cell subset, where they also inhibited degranulation. In contrast, T-MSCs inhibited IFN-γ production in $CD56^{bright}$ NK cells where no obvious receptor expression changes occurred (except for the mild downregulation of NKG2D). Distinct mechanisms may therefore underlie T-MSC-mediated inhibition of cytokine production by $CD56^{bright}$ and degranulation of $CD56^{dim}$ NK cells, with the possible implication of NKG2D in both functions of the two NK subsets.

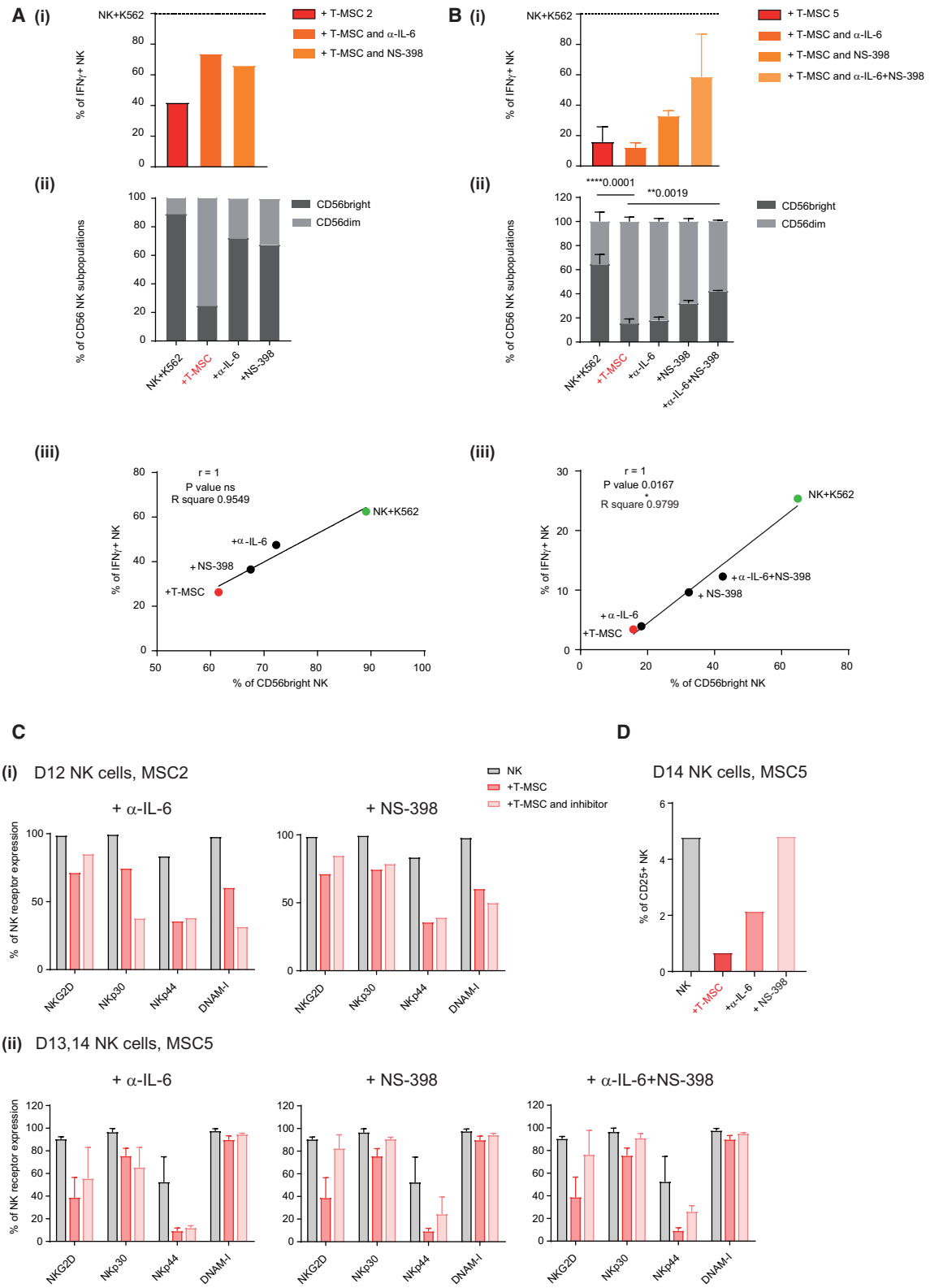

Figure 6. Targeting T-MSC-Derived Immunosuppressive Mediators Rescues NK Cell Activity

Data were analyzed by flow cytometry, and results show mean values ± SEM.

(A) Results are from one rescue experiment with a single NK cell donor and MSCs from patient 2.

(legend continued on next page)

Marked differences in expression and secretion of IL-6 and PGE2 by N- and T-MSCs suggested that both mediators may be implicated in T-MSC-mediated immunosuppression. Interleukin-6 and COX-2 inhibitors revealed that T-MSCs rely on PGE2 to mediate much of their immunosuppressive effect. Accordingly, addition of COX-2 inhibitor to MSC-NK cell co-cultures partially restored NK cell IFN-γ expression, the proportion of $CD56^{bright}$ cells, and NKp30, NKp44, NKG2D, and IL-2Rα expression. COX-2 inhibition in different experiments and using MSCs from different patients consistently restored NK function, suggesting that PGE2 secretion provides an immunosuppressive mechanism common to MSCs, irrespective of their origin.

PGE2 Is a Key Mediator of T-MSC-Dependent Immunosuppression

Bone marrow MSCs have been shown to exert a profound inhibitory effect on NK-cell function, outside of the tumor context, mediated by PGE2, IDO1, and/or TGFβ (Sotiropoulou et al., 2006; Spaggiari and Moretta, 2013; Spaggiari et al., 2008). Our observations suggest that T-MSCs suppress NK cell function primarily by PGE2, as neither TGFβ nor IDO1 were upregulated in T-MSCs. Interestingly, plasma PGE2 levels in NSCLC patients have been found to be elevated compared to healthy subjects (Hidalgo et al., 2002), and high expression of COX-2 in tumor sections of NSCLC has been associated with poor prognosis (Bhooshan et al., 2016; Brown and DuBois, 2004; Khuri et al., 2001). Stimulation of NK cells with PGE2 alone reproduced all of the principal effects of T-MSCs, including inhibition of IFN-γ production, the shift toward the $CD56^{dim}$ phenotype, and down-regulation of NK-cell-activating receptors.

Prostaglandin E2 secretion can occur through an IL-6-dependent mechanism, which has been suggested to provide an anti-inflammatory mediator in arthritis (Bouffi et al., 2010). Abrogation of IL-6 increased PGE2 secretion by MSCs, which may constitute a candidate mechanism to explain why the combined inhibition of both was able to better rescue NK cell function. However, the implication of IL-6 in MSC-mediated NK cell immunomodulation was variable. Whereas in one patient, IL-6 inhibition partially restored NK cell function, the same did not hold true for MSC-inhibited NK cells of another patient. Thus, whereas PGE2 secretion appeared to be a common mediator of immunosuppression by MSCs from different patients, IL-6 seemed to provide a more patient-specific immunosuppressive function. Nevertheless, we identified a novel (possibly context-dependent) role for IL-6 in permitting tumor-subverted MSCs to help establish an immunosuppressive microenvironment that impairs NK cell function.

Taken together, our observations show that, despite the variability of MSCs (including the patient origin of the cells, the stage of the tumor from which they were extracted, and the variable expression of ligands for NK cells) and of donor NK cells (from 14 donors, with variations in the panel of receptors expressed and response to tumor cells), which may influence NK cell activation and the degree of inhibition mediated by MSCs, T-MSCs consistently exert stronger immunosuppression of NK cells than N-MSCs. They also provide a mechanistic explanation for differences between the immunomodulatory potential of T- and N-MSCs and highlight the notion that T-MSCs may largely rely on PGE2 and to a lesser extent on IL-6 to exert their immunosuppressive effects. Selection of immunosuppressive mediators by T-MSCs may be determined by signals derived from the tumor cells or from the microenvironment they condition, which may vary from patient to patient. Efforts to discover drugs that could affect MSC behavior by blocking their inhibitory effects may provide promising options to improve anti-tumor NK cell function.

EXPERIMENTAL PROCEDURES

Primary MSC and Tumor Cell Isolation

MSCs

Fresh primary human tumor samples and adjacent macroscopically normal lung tissue were obtained at surgery from 5 SCC patients at the Centre Hospitalier Universitaire Vaudois (CHUV) (Lausanne) with the approval and according to the guidelines of the Ethics Committee of the Canton de Vaud (project authorization no. 131/12). Patients 1–5 were aged 79, 64, 70, 83, and 74, respectively, at the time of surgery. Patients 1 and 2 were female, and patients 3–5 were male. Pathologic tumor staging varied among patients from T2a to T3 and was performed at the CHUV. T-MSCs and N-MSCs were isolated after tissue disruption (see Supplemental Experimental Procedures) and cultured in Iscove's Modified Dulbecco's Medium (IMDM) supplemented with 10% fetal calf serum (FCS) (PAN-Biotech), 1% penicillin/streptomycin (PS) (Gibco), 1% non-essential amino acids (NEAA) (Gibco), and 10 ng/mL platelet-derived growth factor (PDGF) (Prospec; MSC medium). Cells were used at early passages for all experiments (below p 7). MSCs were assessed for differentiation potential (to osteocytic, chondrocytic, and adipocytic lineages) and membrane expression of selected markers (see Supplemental Experimental Procedures). Fresh human BM-MSCs were obtained from a healthy donor (male donor; 78 years old; project authorization no. 131/12) and harvested as described above.

Tumor Cells

From 3 out of 5 patient samples, PCCs were isolated and cultured as spheres in low-attachment conditions in IMDM supplemented with 20% knockout serum (Gibco), 1% PS, and 20 ng/mL epidermal growth factor (EGF), fibroblast growth factor (FGF), and LIF (Prospec). PCCs were assessed by flow

(B) Summary of two rescue experiments with MSCs from patient 5 (two NK cell donors).

(A and B) (i) Percentage of IFN-γ^+ NK cells after activation by K562 cells in the presence of T-MSCs with or without anti-IL-6-neutralizing antibody and/or NS-398. Results are normalized to NK cell activation by K562 cells in the absence of MSCs, considered to be 100% (horizontal dashed line). (ii) Percentages of K562-activated $CD56^{bright}$ and $CD56^{dim}$ NK subsets cultured alone or with T-MSCs in the presence or absence of inhibitors are shown. Statistical significance was determined by 2-way ANOVA followed by Dunnett's multiple comparisons test, with K562-activated NK cells co-cultured with T-MSCs set as the control (red). (iii) Correlation between the percentage of $CD56^{bright}$ NK cells and intracellular IFN-γ production in different culture conditions is shown. The statistical test used was the Spearman correlation coefficient r, p values are reported, and linear regression line with R square for goodness of fit.

(C) Percentage of NK receptor expression after 4 days in culture alone (gray bar) or with T-MSCs in the absence (dark red bar) or presence of the indicated inhibitors (light red bar). (i) MSC2 is shown; one NK cell donor. (ii) MSC5 is shown; two NK cell donors.

(D) Percentage of IL-2Rα (CD25) expression on NK cells cultured alone (gray bar) or in the presence of T-MSCs (red bars) with or without the indicated inhibitors. Data are representative of a single experiment with a single NK cell donor and MSC5.

See also Figure S5.

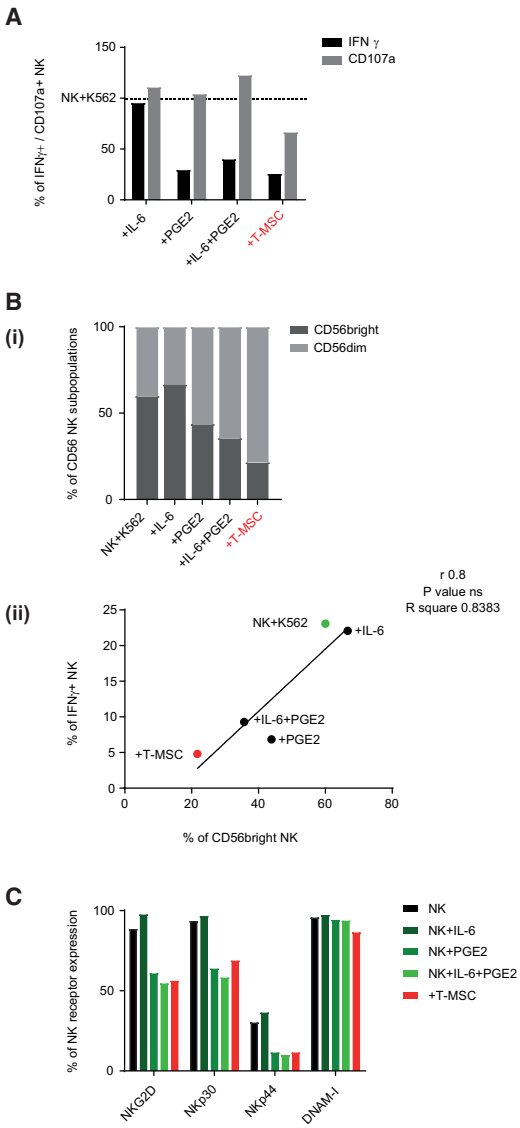

Figure 7. NK Stimulation with PGE2 Mimics MSC-Mediated IFN-γ Immunosuppression

Data were assessed by flow cytometry on NK cells from a single donor. T-MSCs used for co-culture were from patient 5.

(A) Percentages of IFN-γ^+ (black bar) and CD107a$^+$ NK cells (gray bar) after activation by K562 cells in different culture conditions: with IL-6, PGE2, a combination of both, or co-cultured with T-MSCs for 4 days (set as the control condition, red). Results are normalized to 100% as the level of IFN-γ production and CD107a expression by NK cells activated by K562 cells (horizontal dashed line).

(B) (i) Percentages of CD56^{bright} and CD56^{dim} NK subsets after activation by K562 cells under conditions described in (A). (ii) Correlation between the percentages of CD56^{bright} and IFN-γ^+ NK cells is shown. The statistical test used was the Spearman correlation coefficient r, significance determined at $p < 0.05$, and linear regression line and significance determined with R square value.

(C) Percentage of indicated receptor expression on NK cells alone, stimulated with IL-6, PGE2, or both or co-cultured with T-MSCs.

cytometry for HLA-ABC expression (see Supplemental Experimental Procedures). The K562 human leukemia cell line (ATCC no. CCL-243) was cultured in RPMI1640 supplemented with 10% FCS and 1% PS.

Tumor-Infiltrating Immune Cell Characterization

Immune cell infiltration in the tumor bulk was assessed by IHC on whole-tissue sections from SCCs of four patients and by flow cytometry of tumor bulk from three patients after dissociation (see Supplemental Experimental Procedures).

Microscopy

Images were taken with a Nikon Eclipse E800, digital camera DXM1200, at 20× or 40× magnification and at a resolution of 1,280 × 1,024, and analyzed with the ACT-1 (v.2) software.

NK Cell Isolation and Culture

NK cells were isolated from peripheral blood mononuclear cells derived from buffy coats obtained from 14 healthy volunteer donors with donor consent and approval from the Ethics Committee of the Canton de Vaud (project authorization no. P-108). NK cells were cultured in RPMI1640 (Gibco) supplemented with 10% heat-inactivated human serum (Sigma and Life Technologies), 1% PS, and IL-2 (10 ng/mL; R&D Systems; NK medium; see Supplemental Experimental Procedures).

Co-culture Experiments

T-MSCs and N-MSCs were plated in 96-well plates 24 hr before co-culture (0.5×10^5 cells/well). MSCs were treated with mitomycin C 50 μg/mL (Sigma), and freshly isolated NK cells (10^5 cells) were added at 1:2 MSC:NK ratio. Media were supplemented with IL-2 10 ng/mL (R&D). After 4 days of NK-MSC co-culture in NK medium, 10^5 K562 target cells or PCC were added and maintained in co-culture for 4 hr.

Flow Cytometry

See Supplemental Experimental Procedures for more detailed information.

MSC Characterization

Cells were stained with the « human MSC phenotyping kit » (no. 130-095-198; Miltenyi Biotec) according to the manufacturer's protocol.

NK Phenotype

Before and after 4 days of co-culture with MSCs, the NK cell phenotype was assessed using anti-NKp30 (phycoerythrin [PE]; no. 558407; BD Biosciences; 1:50), -NKG2D (antigen-presenting cell [APC]; no. 562064; BD Biosciences; 1:10), -NKG2A (fluorescein isothiocyanate [FITC]; no. 130-098-817; Miltenyi; 1:20), -NKp44 (PE; no. 558563, BD Biosciences; 1:15), -DNAM-I (PE; no. 130-100-461; Miltenyi; 1:20), and -CD25 (APC; no. 555434; BD Biosciences; 1:10) antibodies among CD45$^+$CD3$^-$CD56$^+$CD16$^{+/-}$ cells (anti-CD45 Alexa Fluor 700, no. 560566, BD Biosciences, 1:20; anti-CD3 PC7, no. 41116015, Beckman Coulter, 1:20; anti-CD56 ECD, no. 41116015, Beckman Coulter, 1:40; anti-CD16 PerCP-Cy5.5, no. 560717, BD Biosciences, 1:20).

CD107a Degranulation and Intracellular IFN-γ

After 4 hr activation by target cells, NK cells were stained with anti-CD107a (FITC; no. 555800; BD Biosciences; 1:10), -CD3, -CD45, -CD56, and -CD16 antibodies. Intracellular IFN-γ expression was assessed with APC-conjugated anti-IFN-γ antibody (no. 130-097-944; Miltenyi; 1:25) after cell fixation (PFA) and permeabilization (PBS + BSA 0.2% + saponine 0.1% buffer, for 30 min at room temperature). NK degranulation and IFN-γ expression were quantified within the CD45$^+$CD3$^-$CD56$^+$CD16$^{+/-}$ cell population. NK cells without target tumor cells were used as a control.

Inhibitors/Stimulatory Molecules

Inhibitors

Human anti-IL-6 antibody (MAB206; clone no. 6708; R&D) was added at the final concentration of 2 μg/mL at the start of co-culture. Inhibition of PGE2 was achieved using NS-398 (no. 70590; Cayman Chemical) at the final concentration of 5 μM. Medium + DMSO or + PBS were used as negative controls for NS-398 and IL-6 treatment, respectively.

NK Stimulation

Human recombinant IL-6 (SRP3096; Sigma) was used at a final concentration of 25 ng/mL. PGE2 was obtained from Sigma (P0409) and used at 1 μM

(350 ng/mL). Medium + EtOH was used as a negative control. NK cells were treated for 4 days.

ELISA

IFN-γ ELISA (Human IFN-γ DuoSet ELISA; no. DY285-05; R&D) was performed on MSC/NK/K562 and MSC/NK/PCC co-culture supernatants, according to the manufacturer's instructions. Controls for baseline IFN-γ secretion were supernatants from NK cells alone and NK cells cultured with K562 cells. Samples were diluted 2-fold and analyzed in duplicates.

Quantification of IL-6 secretion by MSCs was performed by ELISA (Human IL-6 DuoSet ELISA; no. DY206-05; R&D) in culture supernatants, according to the manufacturer's instructions. Samples were diluted 4- to 8-fold.

PGE2 was quantified using the Prostaglandin E2 Parameter Assay Kit (no. KGE004B; R&D) according to the manufacturer's protocol. Samples were diluted 3- to 7-fold.

IFN-γ, TNFα, HGF, IL-6, and TGFβ1 were assessed in the co-culture supernatants by Luminex assay (Bio-Plex Pro Human Cytokine/TGFβ; Bio-Rad).

RNA Extraction, cDNA Synthesis, and qRT-PCR

Total RNA was extracted from MSCs using the RNeasy mini Kit (QIAGEN), following standard procedures. cDNA was synthesized by reverse transcription using M-MLV Reverse Transcriptase (Promega) according to the manufacturer's instructions. qRT-PCR amplification was performed using TaqMan Universal PCR mastermix or SYBR Green mix (Applied Biosystems). Samples were analyzed in triplicates (37.5 ng of cDNA/reaction). Data were analyzed by the $2^{-\Delta\Delta Ct}$ method, normalizing threshold cycles first to housekeeping gene expression (*PPIA* [protein phosphatase 1; TaqMan probe; Hs99999904_m1], *GAPDH* [SYBR Green], or *TBP* [SYBR Green]) and then to controls. Primers were purchased from Microsynth AG (see Supplemental Experimental Procedures).

Statistics

Wilcoxon matched-pairs signed rank test was used for nonparametric data and for comparing two matched groups (N- and T-MSCs). Multiple group analysis was performed by 2-way ANOVA test followed by Tukey's multiple comparisons test or Dunnett's multiple comparisons test for nonparametric data. Statistical significance (adjusted p value) of the comparison between BM-MSCs and lung tissue MSCs was determined by an unpaired t test with Welch's correction. For qRT-PCR data, multiple t tests corrected for multiple comparisons using the Holm-Sidak method were used to compare mean expression levels between N- and T-MSCs for each patient. For correlation analysis, the Spearman test was used with the correlation coefficient r. Figures also showed linear regression line with R^2 for the goodness of fit. Calculations were performed in Prism 7 (GraphPad Software). p values < 0.05 were considered statistically significant and are denoted by asterisks: *p < 0.05; **p < 0.01; ***p < 0.001; ns, not significant. Error bars represent the SEM, unless stated otherwise.

ACCESSION NUMBERS

The accession numbers for the data reported in this paper are Flow Repository: FR-FCM-ZYA4; FR-FCM-ZYAE; FR-FCM-ZYAY; FR-FCM-ZYAD; FR-FCM-ZYAC; FR-FCM-ZYAB; FR-FCM-ZYAA; FR-FCM-ZYA9; FR-FCM-ZYA8; FR-FCM-ZYA7; FR-FCM-ZYA6; FR-FCM-ZYA5; FR-FCM-ZYA3; FR-FCM-ZYA2; FR-FCM-ZYAZ; and FR-FCM-ZY9V.

SUPPLEMENTAL INFORMATION

Supplemental Information includes Supplemental Experimental Procedures, five figures, and one table and can be found with this article online at http://dx.doi.org/10.1016/j.celrep.2017.08.089.

AUTHOR CONTRIBUTIONS

Conceptualization, S.G., G.F., and I.S.; Methodology, S.G. and G.F.; Investigation, S.G., G.F., P.M., and J.V.; Writing – Original Draft, S.G.; Writing – Review & Editing, S.G., G.F., A.C., and I.S.; Funding Acquisition, I.S. and S.G.; Resources, I.S. and I.L.; Supervision, G.F. and I.S.

ACKNOWLEDGMENTS

We thank Jean-Christophe Stehle at the Mouse Pathology Facility for assistance with immunohistochemical staining and Prof. Christophe Galland for helpful suggestions. This work was supported by the Swiss National Science Foundation grants 310030_150024 and 310030_169563 (I.S.) and an MD-PhD Fellowship 323630_151474/1 (S.G.).

Received: May 15, 2017
Revised: July 20, 2017
Accepted: August 27, 2017
Published: September 19, 2017

REFERENCES

Aggarwal, S., and Pittenger, M.F. (2005). Human mesenchymal stem cells modulate allogeneic immune cell responses. Blood *105*, 1815–1822.

Alter, G., Malenfant, J.M., and Altfeld, M. (2004). CD107a as a functional marker for the identification of natural killer cell activity. J. Immunol. Methods *294*, 15–22.

Bernardo, M.E., and Fibbe, W.E. (2013). Mesenchymal stromal cells: sensors and switchers of inflammation. Cell Stem Cell *13*, 392–402.

Bhooshan, N., Staats, P.N., Fulton, A.M., Feliciano, J.L., and Edelman, M.J. (2016). Prostaglandin E receptor EP4 expression, survival and pattern of recurrence in locally advanced NSCLC. Lung Cancer *101*, 88–91.

Bouffi, C., Bony, C., Courties, G., Jorgensen, C., and Noël, D. (2010). IL-6-dependent PGE2 secretion by mesenchymal stem cells inhibits local inflammation in experimental arthritis. PLoS ONE *5*, e14247.

Brown, J.R., and DuBois, R.N. (2004). Cyclooxygenase as a target in lung cancer. Clin. Cancer Res. *10*, 4266s–4269s.

Bussard, K.M., Mutkus, L., Stumpf, K., Gomez-Manzano, C., and Marini, F.C. (2016). Tumor-associated stromal cells as key contributors to the tumor microenvironment. Breast Cancer Res. *18*, 84.

Caligiuri, M.A. (2008). Human natural killer cells. Blood *112*, 461–469.

Carrega, P., and Ferlazzo, G. (2017). Natural killers are made not born: how to exploit NK cells in lung malignancies. Front. Immunol. *8*, 277.

Casado, J.G., Tarazona, R., and Sanchez-Margallo, F.M. (2013). NK and MSCs crosstalk: the sense of immunomodulation and their sensitivity. Stem Cell Rev. *9*, 184–189.

Chen, Z., Fillmore, C.M., Hammerman, P.S., Kim, C.F., and Wong, K.-K. (2014). Non-small-cell lung cancers: a heterogeneous set of diseases. Nat. Rev. Cancer *14*, 535–546.

Chretien, A.-S., Le Roy, A., Vey, N., Prebet, T., Blaise, D., Fauriat, C., and Olive, D. (2014). Cancer-induced alterations of NK-mediated target recognition: current and investigational pharmacological strategies aiming at restoring NK-mediated anti-tumor activity. Front. Immunol. *5*, 122.

Cooper, M.A., Fehniger, T.A., and Caligiuri, M.A. (2001). The biology of human natural killer-cell subsets. Trends Immunol. *22*, 633–640.

Cremer, I., Fridman, W.H., and Sautès-Fridman, C. (2012). Tumor microenvironment in NSCLC suppresses NK cells function. OncoImmunology *1*, 244–246.

DelaRosa, O., Sánchez-Correa, B., Morgado, S., Ramírez, C., del Río, B., Menta, R., Lombardo, E., Tarazona, R., and Casado, J.G. (2012). Human adipose-derived stem cells impair natural killer cell function and exhibit low susceptibility to natural killer-mediated lysis. Stem Cells Dev. *21*, 1333–1343.

Desmoulière, A., Guyot, C., and Gabbiani, G. (2004). The stroma reaction myofibroblast: a key player in the control of tumor cell behavior. Int. J. Dev. Biol. *48*, 509–517.

Di Trapani, M., Bassi, G., Ricciardi, M., Fontana, E., Bifari, F., Pacelli, L., Giacomello, L., Pozzobon, M., Féron, F., De Coppi, P., et al. (2013). Comparative study of immune regulatory properties of stem cells derived from different tissues. Stem Cells Dev. *22*, 2990–3002.

Dominici, M., Le Blanc, K., Mueller, I., Slaper-Cortenbach, I., Marini, F., Krause, D., Deans, R., Keating, A., Prockop, Dj., and Horwitz, E. (2006). Minimal criteria for defining multipotent mesenchymal stromal cells. The International Society for Cellular Therapy position statement. Cytotherapy *8*, 315–317.

Dumitru, C.A., Hemeda, H., Jakob, M., Lang, S., and Brandau, S. (2014). Stimulation of mesenchymal stromal cells (MSCs) via TLR3 reveals a novel mechanism of autocrine priming. FASEB J. *28*, 3856–3866.

Esendagli, G., Bruderek, K., Goldmann, T., Busche, A., Branscheid, D., Vollmer, E., and Brandau, S. (2008). Malignant and non-malignant lung tissue areas are differentially populated by natural killer cells and regulatory T cells in non-small cell lung cancer. Lung Cancer *59*, 32–40.

Gillard-Bocquet, M., Caer, C., Cagnard, N., Crozet, L., Perez, M., Fridman, W.H., Sautès-Fridman, C., and Cremer, I. (2013). Lung tumor microenvironment induces specific gene expression signature in intratumoral NK cells. Front. Immunol. *4*, 19.

Gottschling, S., Granzow, M., Kuner, R., Jauch, A., Herpel, E., Xu, E.C., Muley, T., Schnabel, P.A., Herth, F.J.F., and Meister, M. (2013). Mesenchymal stem cells in non-small cell lung cancer–different from others? Insights from comparative molecular and functional analyses. Lung Cancer *80*, 19–29.

Groh, V., Wu, J., Yee, C., and Spies, T. (2002). Tumour-derived soluble MIC ligands impair expression of NKG2D and T-cell activation. Nature *419*, 734–738.

Hidalgo, G.E., Zhong, L., Doherty, D.E., and Hirschowitz, E.A. (2002). Plasma PGE-2 levels and altered cytokine profiles in adherent peripheral blood mononuclear cells in non-small cell lung cancer (NSCLC). Mol. Cancer *1*, 5.

Hodge, G., Barnawi, J., Jurisevic, C., Moffat, D., Holmes, M., Reynolds, P.N., Jersmann, H., and Hodge, S. (2014). Lung cancer is associated with decreased expression of perforin, granzyme B and interferon (IFN)-γ by infiltrating lung tissue T cells, natural killer (NK) T-like and NK cells. Clin. Exp. Immunol. *178*, 79–85.

Imai, K., Matsuyama, S., Miyake, S., Suga, K., and Nakachi, K. (2000). Natural cytotoxic activity of peripheral-blood lymphocytes and cancer incidence: an 11-year follow-up study of a general population. Lancet *356*, 1795–1799.

Jamieson, A.M., Diefenbach, A., McMahon, C.W., Xiong, N., Carlyle, J.R., and Raulet, D.H. (2002). The role of the NKG2D immunoreceptor in immune cell activation and natural killing. Immunity *17*, 19–29.

Jin, S., Deng, Y., Hao, J.-W., Li, Y., Liu, B., Yu, Y., Shi, F.-D., and Zhou, Q.-H. (2014). NK cell phenotypic modulation in lung cancer environment. PLoS ONE *9*, e109976.

Johann, P.-D., Vaegler, M., Gieseke, F., Mang, P., Armeanu-Ebinger, S., Kluba, T., Handgretinger, R., and Müller, I. (2010). Tumour stromal cells derived from paediatric malignancies display MSC-like properties and impair NK cell cytotoxicity. BMC Cancer *10*, 501.

Kalluri, R. (2016). The biology and function of fibroblasts in cancer. Nat. Rev. Cancer *16*, 582–598.

Khuri, F.R., Wu, H., Lee, J.J., Kemp, B.L., Lotan, R., Lippman, S.M., Feng, L., Hong, W.K., and Xu, X.-C. (2001). Cyclooxygenase-2 overexpression is a marker of poor prognosis in stage I non-small cell lung cancer. Clin. Cancer Res. *7*, 861–867.

Krampera, M. (2011). Mesenchymal stromal cell 'licensing': a multistep process. Leukemia *25*, 1408–1414.

Krampera, M., Cosmi, L., Angeli, R., Pasini, A., Liotta, F., Andreini, A., Santarlasci, V., Mazzinghi, B., Pizzolo, G., Vinante, F., et al. (2006). Role for interferon-gamma in the immunomodulatory activity of human bone marrow mesenchymal stem cells. Stem Cells *24*, 386–398.

Lanier, L.L., Le, A.M., Civin, C.I., Loken, M.R., and Phillips, J.H. (1986). The relationship of CD16 (Leu-11) and Leu-19 (NKH-1) antigen expression on human peripheral blood NK cells and cytotoxic T lymphocytes. J. Immunol. *136*, 4480–4486.

Le Blanc, K., and Davies, L.C. (2015). Mesenchymal stromal cells and the innate immune response. Immunol. Lett. *168*, 140–146.

Levi, I., Amsalem, H., Nissan, A., Darash-Yahana, M., Peretz, T., Mandelboim, O., and Rachmilewitz, J. (2015). Characterization of tumor infiltrating natural killer cell subset. Oncotarget *6*, 13835–13843.

Liu, R., Wei, S., Chen, J., and Xu, S. (2014). Mesenchymal stem cells in lung cancer tumor microenvironment: their biological properties, influence on tumor growth and therapeutic implications. Cancer Lett. *353*, 145–152.

Moretta, L., Biassoni, R., Bottino, C., Mingari, M.C., and Moretta, A. (2001). Immunobiology of human NK cells. Transplant. Proc. *33*, 60–61.

Oppenheim, D.E., Roberts, S.J., Clarke, S.L., Filler, R., Lewis, J.M., Tigelaar, R.E., Girardi, M., and Hayday, A.C. (2005). Sustained localized expression of ligand for the activating NKG2D receptor impairs natural cytotoxicity in vivo and reduces tumor immunosurveillance. Nat. Immunol. *6*, 928–937.

Platonova, S., Cherfils-Vicini, J., Damotte, D., Crozet, L., Vieillard, V., Validire, P., André, P., Dieu-Nosjean, M.-C., Alifano, M., Régnard, J.-F., et al. (2011). Profound coordinated alterations of intratumoral NK cell phenotype and function in lung carcinoma. Cancer Res. *71*, 5412–5422.

Poggi, A., and Giuliani, M. (2016). Mesenchymal stromal cells can regulate the immune response in the tumor microenvironment. Vaccines (Basel) *4*, E41.

Poggi, A., Prevosto, C., Massaro, A.-M., Negrini, S., Urbani, S., Pierri, I., Saccardi, R., Gobbi, M., and Zocchi, M.R. (2005). Interaction between human NK cells and bone marrow stromal cells induces NK cell triggering: role of NKp30 and NKG2D receptors. J. Immunol. *175*, 6352–6360.

Poggi, A., Musso, A., Dapino, I., and Zocchi, M.R. (2014). Mechanisms of tumor escape from immune system: role of mesenchymal stromal cells. Immunol. Lett. *159*, 55–72.

Pross, H.F., and Lotzová, E. (1993). Role of natural killer cells in cancer. Nat. Immun. *12*, 279–292.

Raffaghello, L., and Dazzi, F. (2015). Classification and biology of tumour associated stromal cells. Immunol. Lett. *168*, 175–182.

Rasmusson, I., Ringdén, O., Sundberg, B., and Le Blanc, K. (2003). Mesenchymal stem cells inhibit the formation of cytotoxic T lymphocytes, but not activated cytotoxic T lymphocytes or natural killer cells. Transplantation *76*, 1208–1213.

Sotiropoulou, P.A., Perez, S.A., Gritzapis, A.D., Baxevanis, C.N., and Papamichail, M. (2006). Interactions between human mesenchymal stem cells and natural killer cells. Stem Cells *24*, 74–85.

Spaggiari, G.M., and Moretta, L. (2013). Cellular and molecular interactions of mesenchymal stem cells in innate immunity. Immunol. Cell Biol. *91*, 27–31.

Spaggiari, G.M., Capobianco, A., Becchetti, S., Mingari, M.C., and Moretta, L. (2006). Mesenchymal stem cell-natural killer cell interactions: evidence that activated NK cells are capable of killing MSCs, whereas MSCs can inhibit IL-2-induced NK-cell proliferation. Blood *107*, 1484–1490.

Spaggiari, G.M., Capobianco, A., Abdelrazik, H., Becchetti, F., Mingari, M.C., and Moretta, L. (2008). Mesenchymal stem cells inhibit natural killer-cell proliferation, cytotoxicity, and cytokine production: role of indoleamine 2,3-dioxygenase and prostaglandin E2. Blood *111*, 1327–1333.

Stagg, J., and Galipeau, J. (2013). Mechanisms of immune modulation by mesenchymal stromal cells and clinical translation. Curr. Mol. Med. *13*, 856–867.

Turley, S.J., Cremasco, V., and Astarita, J.L. (2015). Immunological hallmarks of stromal cells in the tumour microenvironment. Nat. Rev. Immunol. *15*, 669–682.

Uccelli, A., Moretta, L., and Pistoia, V. (2006). Immunoregulatory function of mesenchymal stem cells. Eur. J. Immunol. *36*, 2566–2573.

Uccelli, A., Moretta, L., and Pistoia, V. (2008). Mesenchymal stem cells in health and disease. Nat. Rev. Immunol. *8*, 726–736.

Villegas, F.R., Coca, S., Villarrubia, V.G., Jiménez, R., Chillón, M.J., Jareño, J., Zuil, M., and Callol, L. (2002). Prognostic significance of tumor infiltrating natural killer cells subset CD57 in patients with squamous cell lung cancer. Lung Cancer *35*, 23–28.

Vitale, M., Cantoni, C., Pietra, G., Mingari, M.C., and Moretta, L. (2014). Effect of tumor cells and tumor microenvironment on NK-cell function. Eur. J. Immunol. *44*, 1582–1592.

Vivier, E., Tomasello, E., Baratin, M., Walzer, T., and Ugolini, S. (2008). Functions of natural killer cells. Nat. Immunol. *9*, 503–510.

Williams, A.R., and Hare, J.M. (2011). Mesenchymal stem cells: biology, pathophysiology, translational findings, and therapeutic implications for cardiac disease. Circ. Res. *109*, 923–940.

Wood, S.L., Pernemalm, M., Crosbie, P.A., and Whetton, A.D. (2014). The role of the tumor-microenvironment in lung cancer-metastasis and its relationship to potential therapeutic targets. Cancer Treat. Rev. *40*, 558–566.

Zaidi, M.R., and Merlino, G. (2011). The two faces of interferon-γ in cancer. Clin. Cancer Res. *17*, 6118–6124.